FR9401663

I. P. N. - 91406 ORSAY CEDEX

institut de physique nucléaire CNRS - IN2P3 UNIVERSITÉ PARIS - SUD

IPNO DRE 93-28

SEPARATION AND IMPLANTATION OF RELATIVISTIC ^{86}Kr-FRAGMENTS AT THE FRS ; HALF-LIFE MEASUREMENT BY ION-β TIME-CORRELATIONS

S. Czajkowski, M. Bernas, IPN, Orsay, France
P. Armbruster, H. Geissel, C. Korshuharov, G, Münzenberg,
D. Vieira, GSI, Darmstadt, Germany
Ph. Dessagne, Ch. Miehe, CRN, Strasbourg, France
E. Hanelt, Technische Hochschule, Darmstadt, Germany
G. Audi, CSNSM, Orsay, France
J.K.P. Lee, FRL, MacGill University, Montreal, Canada

IPNO DRE 93-28

SEPARATION AND IMPLANTATION OF RELATIVISTIC ^{86}Kr-FRAGMENTS AT THE FRS ; HALF-LIFE MEASUREMENT BY ION-β TIME-CORRELATIONS

S. Czajkowski, M. Bernas, IPN, Orsay, France
P. Armbruster, H. Geissel, C. Korshuharov, G, Münsenberg,
D. Vieira, GSI, Darmstadt, Germany
Ph. Dessagne, Ch. Miehe, CRN, Strasbourg, France
E. Hanelt, Technische Hochschule, Darmstadt, Germany
G. Audi, CSNSM, Orsay, France
J.K.P. Lee, FRL, MacGill University, Montreal, Canada

Separation and Implantation of Relativistic ^{86}Kr-Fragments at the FRS; Half-Life Measurement by Ion–β Time-Correlations

S. Czajkowski, M. Bernas
Institut de Physique Nucléaire, Orsay, France

P. Armbruster, H. Geissel, C. Kozhuharov, G. Münzenberg, D. Vieira
Gesellschaft für Schwerionenforschung, Darmstadt, Germany

Ph. Dessagne, Ch. Miehe
Centre de Recherche Nucléaire, Strasbourg, France

E. Hanelt
Technische Hochschule, Darmstadt, Germany

G.Audi
CSNSM, Laboratoire René Bernas, Orsay, France

J.K.P. Lee
Foster Radiation Laboratory, MacGill University, Montreal, Canada

27 October 1993

Abstract

Neutron-rich Co and Fe isotopes produced by ^{86}Kr projectile fragmentation at 500 MeV/u have been separated and identified using the Fragment Separator (FRS) in a bunched energy mode. ^{66}Co and ^{65}Fe ions were selectively implanted in a double PIN-diode array where the β-decay signals were measured. The half-lives were deduced from time correlations between implantation and β-decay signals. The re-measurement of the ^{66}Co half-life confirms the isotope identification. The value of ^{65}Fe half-life was found to be 0.45 ± 0.15 s.

PACS: 23.40.-s, 27.50.+e, 29.30.Cm

1 Introduction

Heavy ion projectile fragmentation first observed at the Bevalac [1] has been effective to generate new isotopes far from stability. The many experimental investigations performed over the last 10 years have lead to continuous improvements of the pioneer description of the process in terms of the abrasion-ablation model [2].

The high energy of the ion beams delivered by the new SIS at GSI is extremely suitable for those studies since the reaction kinematics concentrates fragments within a narrow forward cone in a small velocity range, close to the projectile velocity. Therefore the fragments can be efficiently separated within a small solid angle and a narrow momentum aperture even with targets as thick as 1 g/cm^2.

A crucial point for the separation of n-rich rare isotopes comes from the complete ionization of all the elements with $Z < 36$ produced at such high energy. If they were not, even a small fraction of not totally stripped lighter isotopes—more abundant by orders of magnitude—would be contaminants, having the same magnetic rigidity.

The fragment separator (FRS) [3] is presently a unique instrument for studying the neutron rich isotopes beyond mass $A = 60$. The study of those isotopes is of great interest to test nuclear models far off stability mainly along the $Z = 28$ shell or $N = 40$ subshell. Furthermore these nuclei are encountered at the beginning of the astrophysical r-process path, following the very first neutron captures on the seed nucleus ^{56}Fe. The β decay half-lives of these nuclei, especially those close to the $N = 50$ line, are required in order to calculate the r-process features and to narrow down the uncertainties on the astrophysical parameters related with this process.

In this work [4] the FRS was tuned to separate ^{65}Fe fragments produced in collisions of ^{86}Kr at 500 MeV/u with a Be target. This measurement was part of a series of pilot experiments initiated with the beam of ^{86}Kr. It was the first step for a systematic investigation in the $Z = 22$ to 28 region. A second issue was a demonstration of the FRS performances with a monoenergetic degrader [5]. It has been shown that, in agreement with the foreseen specifications of the instrument, the energy of fragments can be bunched by shaped matter placed in the dispersive central focal plane, so that they can be selected by their range. The yield of exotic species surviving the passage through a substantial thickness of slowing down material is still large enough for spectroscopic studies.

2 Experimental Set-up

The ^{86}Kr ions were delivered at an energy of 500 MeV/u by the GSI heavy ion synchrotron (SIS). 60 ms spills of 5.10^7 particles were directed every 3s on a Be target at the entrance of the F R S.

2.1 Magnetic Selection

The FRS [3] consists mainly of two magnetic stages symmetric with respect to a dispersive focal plane (S2). Each stage combines two identical sections consisting of one dipole, a quadrupole

triplet and a quadrupole doublet in order to optimize the optical properties for reaction studies with an appropriate versatility. Given the kinematics of projectile fragmentation, magnetic deflection separates isotopes with similar A/Z ratio. An additional selection is realized by introducing an energy degrader in the dispersive plane. The shape of the degrader can be adjusted to preserve the achromatism of the whole system for a desired fragment.

To obtain the so-called monoenergetic mode, the angle of the wedge degrader is enlarged until to compensate the momentum spread for the fragment of interest. Thus for this fragment the different energies are bunched independently of the position they had in the plane S2. Fragments can be analyzed by the second stage of the FRS keeping an extended horizontal image, presently covering 15 cm. The vertical focusing over 0.4 cm was unchanged compared to the achromatic regime. As the desired fragments have a well defined energy, they can be further separated due to this property.

2.2 Target and Degrader

The target material and thickness were chosen to optimize the count rates of fragments separated with the FRS. The Be as target provides the maximum number of nuclei inducing fragmentations for a given energy broadening of the merging fragments. The thickness of 2 g cm^{-2} corresponds to 20 % of the range of the primary beam and generates a 3.2 % momentum spread for Fe-Co fragments, which is larger than the FRS momentum acceptance.

All the isotopic yields of the ^{86}Kr + Be, 500 MeV/u fragmentation reaction were systematically measured in another experiment[6].

The variable thickness of the intermediate Al wedge, remotely controlled was taken to be 6.5 g.cm^{-2}, i.e., 55 % of the ^{65}Fe range. This was chosen in order to increase the range differences between ^{65}Fe and ^{65}Co or ^{64}Fe contaminants and to decrease the last degrader thickness. The angle of the wedge was adjusted to 17.8 mr. The settings (fig. 1) were calculated using the kinematical code "LIESCHEN"[7]. In the second magnetic stage, the energy of the ^{65}Fe ions was 300 MeV/u. An additional homogeneous Al-degrader of adjustable thickness placed at the exit of the F R S, slows them down to the energy of 20 MeV/u required for implantation in the detecting device.

Unwanted secondary atomic and nuclear reactions are taking place in both energy degrader. They reduce the transmission efficiency and add angular and energy straggling. Nuclear secondary reactions in the last homogeneous degrader generate particle background in our detecting system. Therefore, it was appropriate to reduce the fraction of the energy loss in the last degrader. In the total material thickness of approximately 9 g cm^{-2}, the proportion of ^{65}Fe transmitted without secondary reactions is calculated to be 40 %.

2.3 ΔE-TOF Measurements

The identification of the selected fragments was performed with the standard FRS detectors; the energy loss measurements in a MUSIC chamber [8] provides the atomic charge Z. The time of flight of fragments was measured along the 35 m path between a PPAC located in the intermediate focal

plane S2 and a plastic scintillator in the final focal plane S4 (Fig. 1). With the wedge thickness and the FRS setup given in fig. 1 three elements with three masses number each were transmitted. Simulations were performed with the code MOCADI [9]. They provided the expected scatter-plot (ΔE-TOF) and the transmission efficiencies for the 9 fragments.

2.4 Implantation Setup

The set-up consists of two parallel rows of 10 Si PIN-diodes of 120 mg.cm^{-2}, (500 μm) thickness (Fig. 2). The surface of each diode is 1 x 1 cm^2 and they are mounted close to each other, thus 11 cm of the focal plane in S4 are covered. The position information for ions and β particles is exploited to reject random coincidences.

Located behind a plastic scintillator of 16 x 6 cm^2 and 5 mm thickness provides a veto for more penetrating particles or secondary fragments. The energy deposited by fragments, stopped in the diode, is 20 MeV/u, i.e., 1.2 GeV while the energy loss of the β particle is only of the order of 100 keV, depending on its trajectory in the diode. To process those two signals, four orders of magnitude apart, two read-out chains were required down to the preamplification: Compact packages of charge-sensitive preamplifiers "EXOPAC" were manufactured by the Electronic Services-IPN Orsay- with appropriate feedbacks.

3 Results

3.1 Fragment Identification

The ΔE-TOF scatter plots of fragments selected with the FRS are shown in Fig. 3; in frame a) is shown a net of lines corresponding, to equal values of range, R_i, of energy, E_i, and atomic number, Z_i, with the index indicating increasing values. They were calculated with ion optical simulation code MOCADI. on part b) the gross amount of fragments coming out in S4 is shown; on part c) the fraction of these fragments which have triggered the PIN-diodes: short range fragments are stopped in the last degrader. On part d), the condition from the veto-counter behind the PIN-diodes is added, suppressing 80 % of more penetrating ions. Finally three groups of fragments were selectively implanted, two of which with similar range are isotones. The FRS was set (fig. 1) to select ^{65}Fe, on the Z_2, R_2 lines(Fig. 3).

3.2 Fragment Implantation

From the FRS, to the PIN-diode device, transmissions of 4 % and 2 %, for ^{66}Co and ^{65}Fe respectively, were obtained with alignment and focusing being optimized. This low transmission which results from the angular straggling introduced by the last energy degrader can be easily improved in the next measurements. The losses were so large in this measurements only because the PIN-diode detectors had to be set too far apart from the degrader. The count rate of the main implanted group (R_2, Z_3) ^{66}Co, is shown on Fig. 4 as a function of the last energy degrader thickness. The width of the distribution equals the 120 mg cm^{-2} PIN diode thickness. It shows

that the contribution of the range straggling is much less than 120 mg cm^{-2} in agreement with theoretical calculations. More than 35 % of a given fragment can be implanted in a PIN-diode thickness with the FRS tuned in the isorange mode.

If the FRS would have been tuned in the usual achromatic mode, the range spread associated with the momentum acceptance would have been 450 mg cm^{-2}.

3.3 β-Detection

The energy loss signals of β particles in 500 μm Si can be very low and must be detected unambiguously. It was shown in our previous measurement [10] that the accuracy of the half-life measurement depends on optimization of the ratio ε^2/b where ε is the β detection efficiency and b the background rate. In the present case, the energy loss spectrum of β particles, N(ΔE), decreases steadily with ΔE since the fragment implantation depth and the β direction are randomly distributed. The good energy resolution of the pin-diode must be preserved to recognize small signals from noise. With the "EXOPAC" preamplifiers, a resolution of 2.5 % was measured using a ^{207}Bi source. The background counted between the beam pulses without implants, is extremely low; b = 0.035/s/det.

A first estimate of $\varepsilon \sim 60\%$ is obtained from the ratio of β counting (background excluded) over the number of implants. The factor ε^2/b is therefore large enough ($\sim$ 100) for measuring half-lives up to the time interval between two pulses, 3 s.

3.4 Time Correlations

The probability for finding the first β after the fragment implantation at a time t is given by

$$\rho_1(\lambda,t) = \varepsilon(b+\lambda)e^{-(b+\lambda)t} + (1-\varepsilon)be^{-bt} \quad (1)$$

and in case the daughter decay is included:

$$\rho_1(\lambda,\lambda_f,t) = \rho_1(\lambda,t) + \varepsilon(1-\varepsilon)e^{-bt}\left\{\frac{\lambda\lambda_f}{\lambda-\lambda_f}\left(\left[1+\frac{b}{\lambda_f}\right]e^{-\lambda_f t} - \left[1+\frac{b}{\lambda}\right]e^{-\lambda t}\right) - b\right\} \quad (2)$$

For the implant with the main counting rate (R_2, Z_3) least square fit and maximum likelihood methods [10] lead to a half-life value of (0.24 $\pm$ 0.03) s Given the pattern of half-lives of isotopes close to ^{65}Fe, this determination confirms the identification of this fragment as ^{66}Co.

The decay of the daughter nuclei, ^{66}Ni, does not interfere since it is very slow ($T_{1/2}$ = 55 h). In Fig. 5a, the ^{66}Co event numbers are plotted as a function of the logarithm of time intervals. The background is low and, thus, the spectrum is clearly split up in 2 contributions; one from the decay and one from the background. Both components are fitted with the standard function xe^{-x} with $x = (b+\lambda)t$ and bt, respectively. This method [11] provides an accurate determination of b and—as a by-product— the β-detection efficiency, ε = 0.65. At very short time intervals, t ¡ 10 ms, a background component related to the high rate of ions from beam pulses is distinctly separated.

For ^{65}Fe time correlations, (Z_2, R_2) group of Fig.3 , the methods mentioned above were used including equation (2), since the daughter decay of ^{65}Co, $T_{1/2}$ = 1.25 s [12] is short enough and could be detected; The half-life obtained (0.4 ± 0.25) s is used to calculate the curve shown in Fig. 5b. Very convincing is the time analysis for sequential β decays. The mean values of time intervals between a fragment detection and the first β decay, t_1, and between the first and the second β decay, t_2, were evaluated: $< t_1 >$ = 0.62 s, and $< t_2 >$ = 1.62 s. They lead to half-life values of (0.45 ± 0.15) s and (1.12 ± 0.25) s, respectively.

The number of 14 β chains selected over the n = 26 implants of ^{65}Fe is consistent with the expectation value of ε^2n ∼ 12.

The detection of sequential β decays gives a high level of confidence for this result in spite of the low statistics. The adopted value for ^{65}Fe half-life is (0.45 ± 0.15) s.

4 Discussion

Initiated and developed for very low count rates of fission fragments [13], the implantation method for β decay half-life measurements has been transferred and adapted for high energy projectile fragmentation using the monoenergetic tuning of the FRS and an additional range selection.

It is worth to compare the conditions of the "isorange" implantation where fragments are spatially distributed over 12 cm, with an implantation of one focused fragment, obtained by an achromatic tuning, in a stack of 4 to 5 similar pin-diodes.

a) The half-lives of two fragments were simultaneously measured, one of which was known. It confirmed that the FRS tuning and range selection were appropriate and it provided reference values of the parameters ε and b.

b) There was no particle, neither electronic cross-talking between the detectors.

c) The granularity of our PIN-diode device reduces the background by a factor 20 for time-correlated events.

Thanks to this very low background the measurement of sequences of β decays has been shown to be very powerful. This method of half-life determination can be further exploited for the new fission fragments discovered in high energy ^{238}U collisions [14] where characteristic long β decay chains are expected. The method was successful, albeit the transmission of fragments of this pilot experiment was very low. With a collection efficiency and transmission of 50 % it is clear that, in the same experimental conditions, projectile fragments of Fe-isotopes heavier by at least two mass units are still measurable, given the production yield distribution [6]. It is worth that β-delayed neutrons cannot be used for $T_{1/2}$ measurements since P_n values are lower than 2%.

The value of 0.45 s presently obtained for ^{65}Fe half-life is smaller than the 2.22 s predicted by the revised gross theory [15] and 3.71 s from microscopic calculations [16]. A similar trend was observed for ^{63}Fe [17], ^{64}Fe [12] and ^{68}Fe [13] as for n-rich Co and Mn isotopes. The $T_{1/2}$ values depend on Q_β as strongly as $(Q_\beta)^5$, thus they emphasize the discrepancies between theory and experiment on binding energies. The above models are used to generate firstly binding energies and then half-lives, over the whole chart of nuclei. Expected half-lives could be improved if experimental Q_β values were included whenever they have been measured. Even with the Liran-

Zeldes binding energy extrapolation, which reproduces the experimental values in the domain under study, the Q_β are underestimated and, therefore half-lives are overestimated. A more recent calculation in the frame of the QRPA approximation [18] has provided shorter half-lives for the quoted isotopes, by using the same mass formulae as TDA calculations of Ref. [17]. However, in that case, the value found for ^{68}Co becomes too short by a factor of 4. To summarize, the calculation of β decay half-lives remains a challenge for test of nuclear models and mass formulae and the measurements of basic nuclear constants such as $T_{1/2}$ and Q_β remains necessary.

5 Conclusion

The measurement of the ^{65}Fe half-life reported here is a first step on a way of studies by a new method to investigate n-rich nuclei properties. In his study of projectile fragmentation of 500 MeV/u ^{86}Kr on Be, Weber et al. [6] observed some 400 different nuclear species. Between Ca and Fe, the production rates are sufficiently high for having 2 to 3 new n-rich isotopes for each element produced with similar rates as ^{66}Co here. Their half-lives are essential for the understanding the astrophysical r-process and can also help to test further nuclear models. Measurements of binding energies and neutron emission probabilities would help as well. Masses are planned to be measured after a transfer of the beam of radioactive isotopes to the storage ring ESR. Since these elements are not easily extracted from on-line mass-separator ion-sources, the coupling of projectile fragmentation with a dedicated in-flight separation technique represents a good method to study these isotopes at the limit of our present knowledge.

References

[1] Symons, T.J.M., Viyogi, Y.P., Westfall, G.D., Doll, P., Greiner, D.E., Faraggi, H., Lindstom, P.J., Scott, D.K., Crawford, H.J., McParland, C.: Phys. Rev. Lett. **42**, 40 (1979) and Westfall, G.D., Symons, T.J.M., Greiner, D.E., Heckmann, H.H., Lindstom, P.J., Mahoney, J., Scott, D.K., Crawford, H.J., McParland, C., Awes, T.C., Gelbke, C.K., Kidd, J.M.: Phys. Rev. Lett. **43**, 1859 (1979)

[2] Goldhaber, A.S.: Phys. Lett. B**53**, 306 (1974)

[3] Geissel, H., Armbruster, P., Behr, K.H., Brünle, A., Burkard, K., Chen, M., Folger, H., Franczak, B., Keller, H., Klepper, O., Langenbeck, B., Nickel, F., Pfeng, E., Pfützner, M., Roeckl, E., Rykaczewski, K., Schall, I., Schardt, D., Scheidenberger, C., Schmidt, K.H., Schröter, A., Schwab, T., Sümmerer, K., Weber, M., Münzenberg, G., Brohm, T., Clerc, H.G., Fauerbach, M., Gaimard, J.J., Grewe, A., Hanelt, E., Knödler, B., Steiner, M., Voss, B., Weckenmann, J., Ziegler, C., Magel, A., Wollnik, H., Dufour, J.P.: Nucl. Instr. Meth. B**70**, 286 (1992)

[4] Czajkowski, S: Ph. D. Thesis, Université Paris VII, Report IPNO T92-02 (1992)

[5] Geissel, H., Schwab, T., Armbruster, P., Dufour, J.P., Hanelt, E., Schmidt, K.H., Sherill, B., Münzenberg, G.: Nucl. Instr. Meth. A**282**, 247 (1989)

[6] Weber, M., Donzaud, C., Dufour, J.P., Geissel, H., Grewe, A., Guillemaud-Mueller, D., Keller, H., Lewitowicz, M., Magel, A., Mueller, A.C., Münzenberg, G., Nickel, F., Pfützner, M., Piechaczek, A., Pravikoff, M., Roeckl, E., Rykaczewski, K.,Saint-Laurent, M.G., Schall, I., Stephan, C., Sümmerer, K., Tassan-Got, L., Vieira, D.J., Voss, B.: Z. Phys. A **343**, 67 (1992)

[7] Hanelt, E., Schmidt, K.H.: Nucl. Instr. Meth. A**321**, 434 (1992)

[8] Pfützner, M., Voss, B., Clerc, H.G., Geissel, H., Münzenberg, G., Nickel, F., Schmidt, K.H., Steiner, M., Sümmerer, K., Vieira, D.J.: GSI Sci. Rep. 1990, GSI 91-1 (1991), p.288

[9] Schwab, Th.: Ph. D. Thesis (universität Gießen), Report GSI 91-10 (1991)

[10] Bernas, M., Armbruster, P., Bocquet, J.P., Brissot, R., Faust, H., Kozhuharov, C., Sida, J.L.: Z. Phys. A **337**, 41 (1990)

[11] Schmidt, K.H., Sahm, C.C., Pielenz, K., Clerc, H.G.: Z. Phys. A **316**, 19 (1984)

[12] Bosch, U., Schmidt-Ott, W.D., Tidemand-Peterson, P., Runte, E., Hillebrandt, W., Lechle, M., Thielemann, F.K., Kirchner, R., Klepper, O., Roeckl, E., Rykaczewski, K., Schardt, D., Kaffrell, N., Bernas, M., Dessagne, Ph., Kurcewicz, W.: Phys. Lett. B **164**, 22 (1985)

[13] Bernas, M., Armbruster, P., Czajkowski, S., Faust, H., Bocquet J.P., Brissot, R.: Phys. Rev. Lett. **67**, 3661 (1991)

[14] Armbruster, P., Bernas, M., Czajkowski, S., Dessagne, Ph., Donzaud, C., Faust, H., Geissel, H., Hanelt, E., Hesse, M., Heinz,A., Kozhuharov, C., Miehe, Ch., Münzenberg, G., Pfützner, M., Röhl, C., Schmidt, K.H., Schwab, W., Stephan, C., Sümmerer, K., Tassan-Got, L., Voss, B.: GSI Sci. Rep. 1992, GSI 93-1 (1993), p.28

[15] Tachibana, T., Yamada, M., Nakata, K.: Report of Sciences and Engineering Research Laboratory 88-4, Wasada University (1988)

[16] Klapdor, H.V., Metzinger, J., Oda, T.: At. Data Nucl. Data Tables **31**, 81 (1984)

[17] Runte, E., Gippert, K.L., Schmidt-Ott, W.D., Tidemand-Peterson, P., Ziegeler, L., Kirchner, R., Klepper, O., Larsson, P.O., Roeckl, E., Schardt, D., Kaffrell, N., Peuser, P., Bernas, M., Dessagne, Ph., Langevin, M.: Nucl. Phys. A441, 237 (1985)

[18] Staudt, A., Bender, E., Muto, K., Klapdor, H.V.: At. Data Nucl. Data Tables 44, 79 (1990)

Figure Captions

Fig. 1: General FRS setup.

Fig. 2: Detecting setup for ion-β time correlations

Fig. 3: Fragments selected with the FRS: **(a)** gross amount of fragments separated by the FRS; **(b)** scheme of isoenergy, isorange, and element lines; **(c)** same fragments triggered by the PIN-diodes; **(d)** same as c) but with the veto scintillator active, i.e. fragments implanted in the PIN-diodes.

Fig. 4: Implantation rate as a function of the degrader thickness for ^{66}Co.

Fig. 5: Histograms of times between the implant and first β detection for ^{66}Co and ^{65}Fe. The low background level b allows a clear separation of the decay from background components.

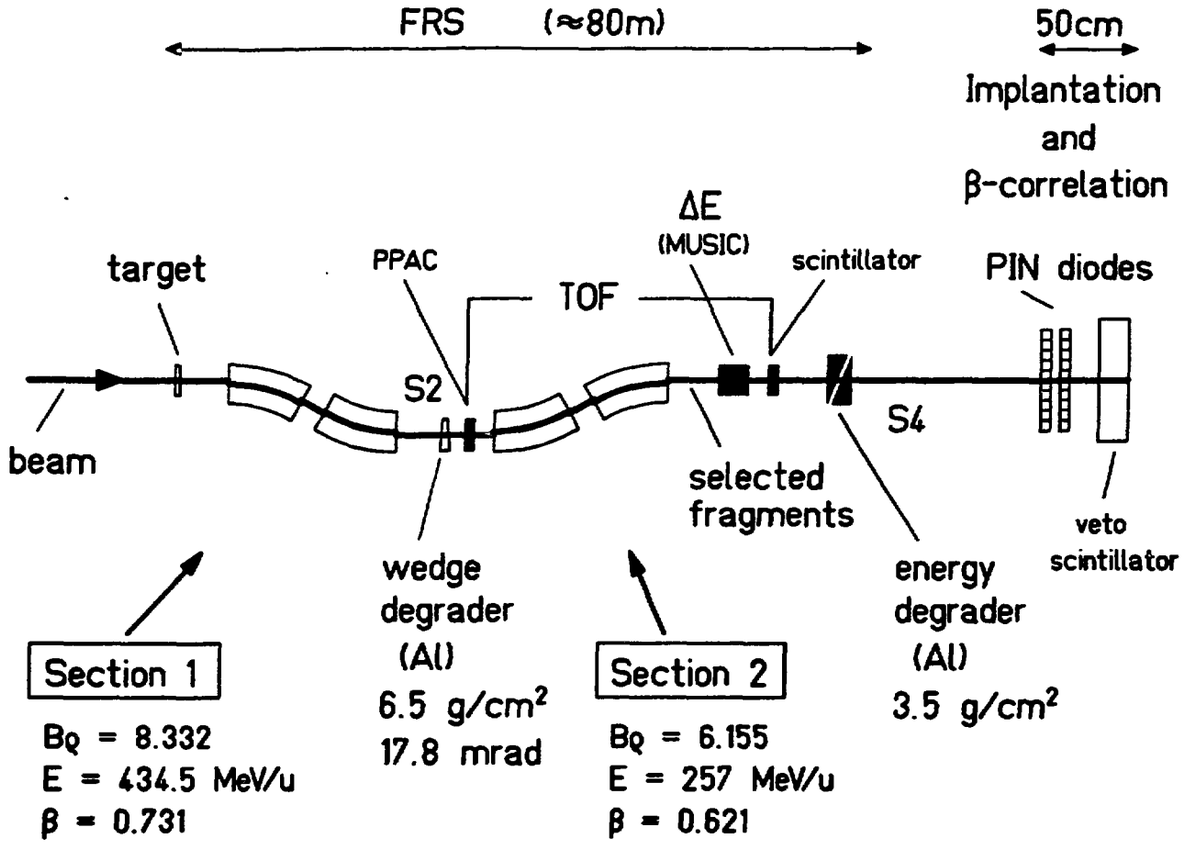
FRS (≈80m)
50cm
Implantation
and
β-correlation
ΔE
(MUSIC)
target
PPAC
TOF
scintillator
PIN diodes
S2
S4
beam
selected
fragments
veto
scintillator
wedge
degrader
(Al)
6.5 g/cm²
17.8 mrad
energy
degrader
(Al)
3.5 g/cm²
Section 1
Bρ = 8.332
E = 434.5 MeV/u
β = 0.731
Section 2
Bρ = 6.155
E = 257 MeV/u
β = 0.621

Fig. 1

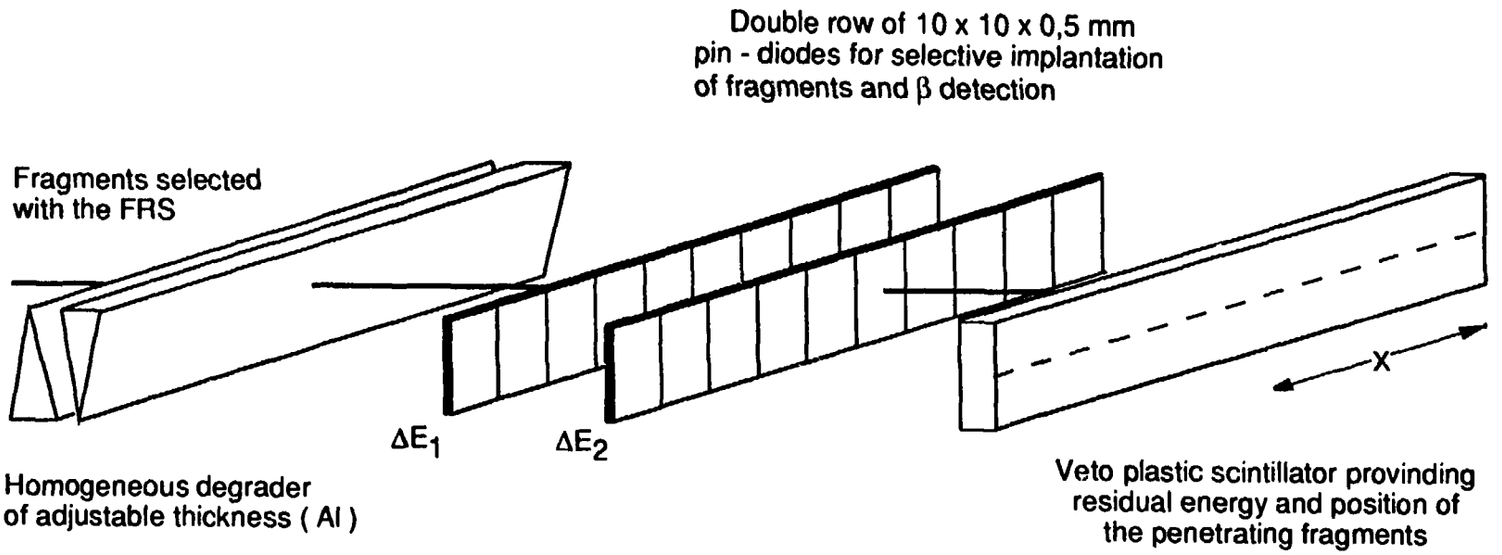
Double row of 10 x 10 x 0,5 mm
pin - diodes for selective implantation
of fragments and β detection
Fragments selected
with the FRS
ΔE1
ΔE2
x
Homogeneous degrader
of adjustable thickness (Al)
Veto plastic scintillator provinding
residual energy and position of
the penetrating fragments

Fig. 2

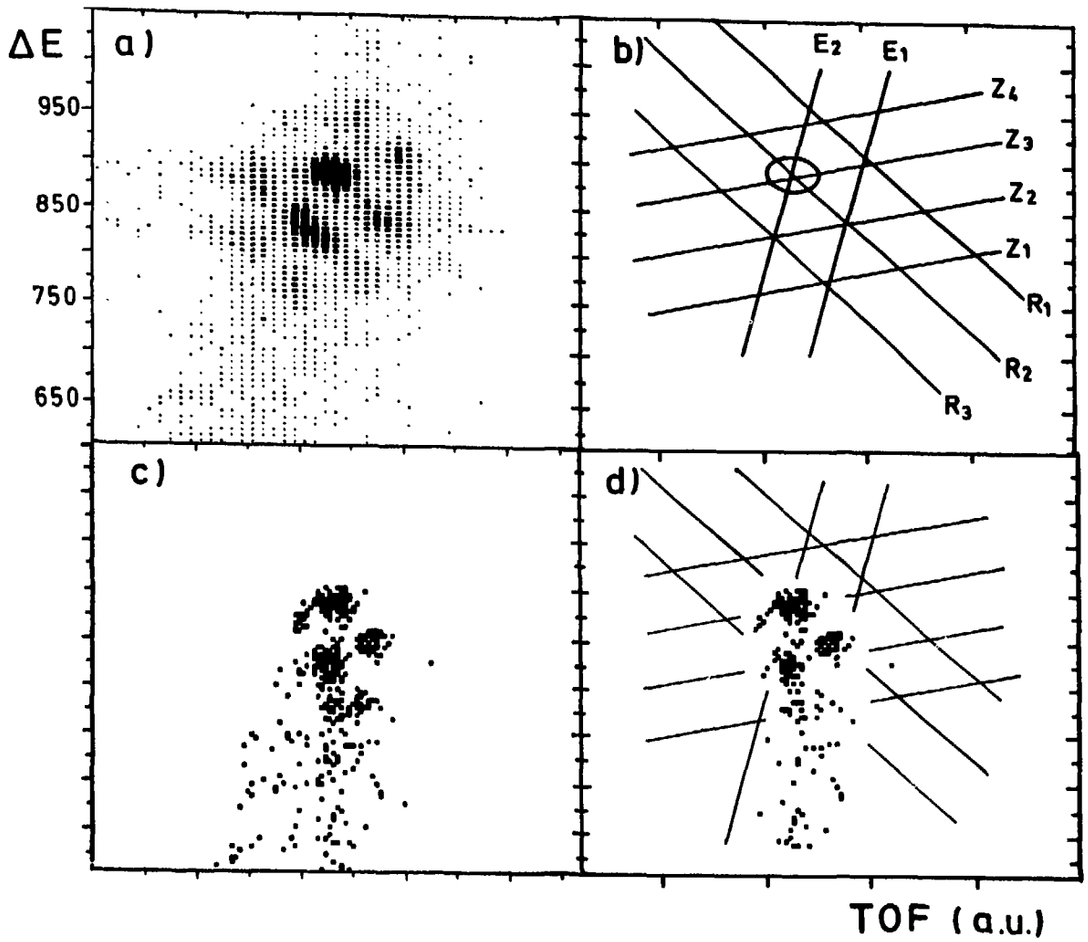
ΔE
a)
950
850
750
650
b)
E2
E1
Z4
Z3
Z2
Z1
R1
R2
R3
c)
d)
TOF (a.u.)

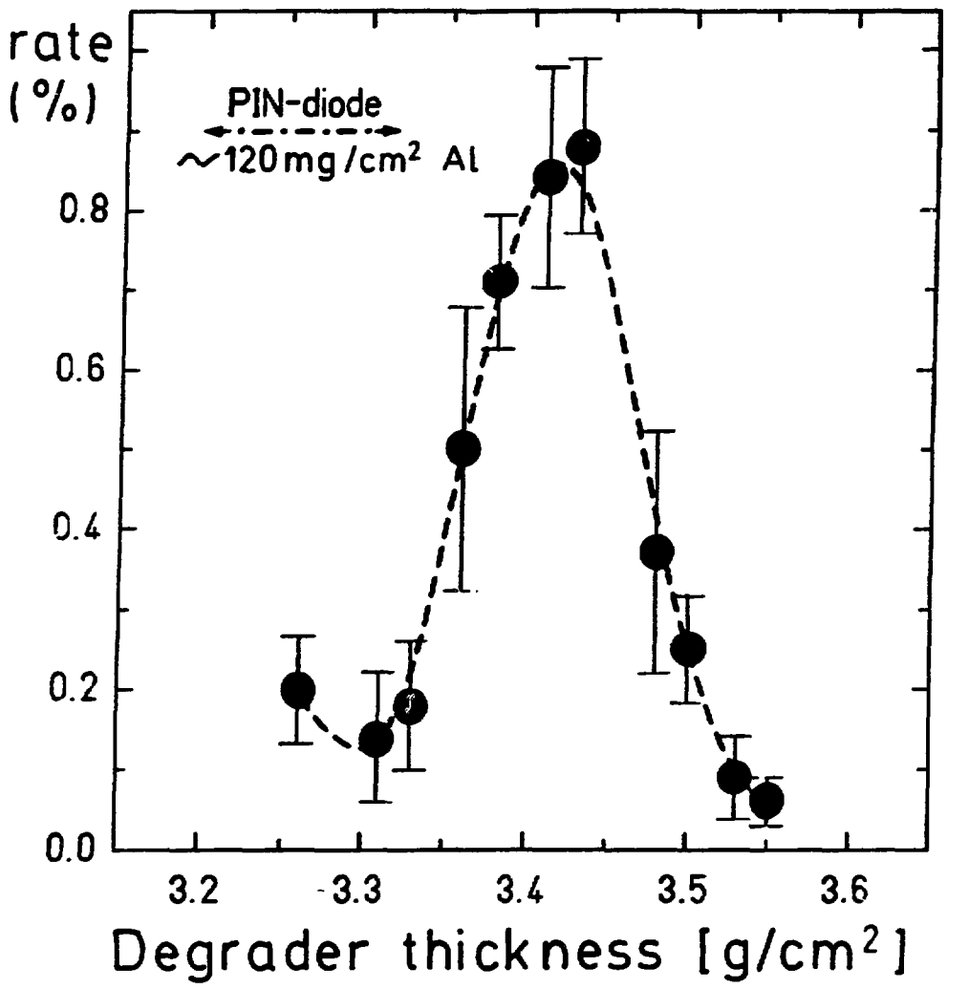
rate
(%)
PIN-diode
~120 mg/cm² Al
0.8
0.6
0.4
0.2
0.0
3.2
3.3
3.4
3.5
3.6
Degrader thickness [g/cm²]

Fig 4

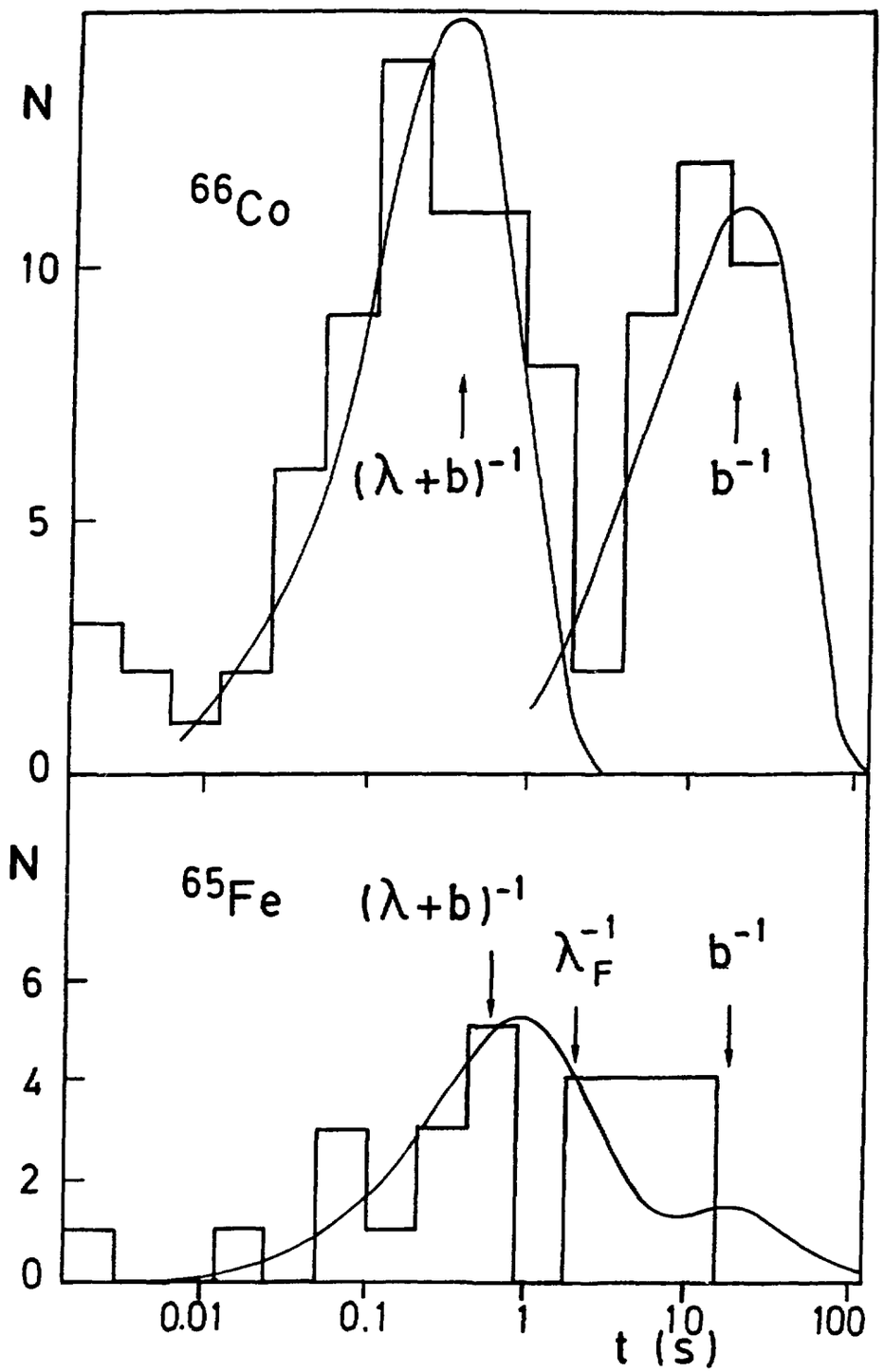
N
^{66}Co
10
5
0
$(\lambda+b)^{-1}$
b^{-1}
N
^{65}Fe
$(\lambda+b)^{-1}$
λ_F^{-1}
b^{-1}
6
4
2
0
0.01
0.1
1
10
100
t (s)

Fig. 5